# Orientation-Fields Segmentation Based on the Notion of Line-Segment Function

Luis A. Morales-Hernández
Universidad Autónoma de Querétaro
Facultad de Ingeniería,
76000 , Querétaro, México
luismorah@yahoo.mx

Iván R. Terol-Villalobos
CIDETEQ
Sanfandila-Pedro Escobedo 76700
Querétaro, México
famter@ciateq.net.mx

Gilberto Herrera-Ruiz
Universidad Autónoma de Querétaro
Facultad de Ingeniería,
76000 , Querétaro, México
gherrera@uaq.mx

## Abstract

*In the present paper a morphological approach for segmenting orientation fields is proposed. This approach is based on the concept of the line-segment and orientation functions. The line-segment function is computed from the supremum of directional erosions. This function contains the sizes of the longest lines that can be included in the structure. To determine the directions of the line segments, the orientation function which contains the angles of the line segments it is built when the line-segment function is computed. Next, by combining both images, permits the construction of a weighted partition using the watershed transformation. Finally, the elements of the partition are merged according to some directional and size criteria for computing the desired segmentation of the image using a RAG structure.*

## 1. Introduction

Anisotropic structures are frequently found in many classes of images (materials, biometry images, biology, ...),however, few works dealing with directional analysis in morphological image processing have been carried out [17, 16, 6, 12, 11] among others. It is maybe in the domain of fingerprint recognition, which is today the most widely used biometric features for personal identification, where the study of directional structures based on orientation-fields detection is an active subject of research [3, 13, 9]. In fact, fingerprints can be considered as a structure composed by a set of line segments (see Fig. 1(a)). However, orientation-field detection also plays a fundamental role in other domains [8, 1, 7]. Lee et *al* [8] propose a method based on oriented connectivity for segmenting solar loops, while Kass and Witkin [7] propose a method to analyze oriented patterns in wood grain. Given the interest in orientation pattern models for characterizing structures, this paper investigates the use of the mathematical morphology for modelling orientation fields. As in the human vision, computer image processing of oriented image structures often requires a bank of directional filters or template masks, each of them sensitive to a specific range of orientations [17]. Then, one investigates the use of an approach based on directional erosions. In the literature there exist several works to characterize directional structures based on the gradient computation that can be formalized in terms of mathematical morphology. See for example the works of [7, 2, 9]. The problem of the gradients is that they work at pixel scale, they are very sensitives to noise and a final stage to enhance directional field is required. Then, the main idea in this paper is focused on another approach that permits to take into account the whole context of the structures contained in the image. That means, a local approach using the concept of line-segment function combined with the watershed transformation is used. In our case, the line-segment function is computed from the supremum of directional erosions. This function contains the information of the longest line segments that can be placed inside the structure. In order to know their orientations, a second image is defined by observing the construction of the line-segment function and its evolution. This second image is computed by detecting the orientation of the supremum of directional erosions. These local descriptors, for the element size and orientation, enable the identification of the orientation fields based

on the watershed transformation. This paper is organized as follows. In Section 2, the concepts of morphological filter and directional morphology are presented. In Section 3 the notions of line-segment and orientation functions, derived from the supremum of directional erosions, are introduced. Next, in Section 4 an approach of working with directional morphology, the watershed transform and a region adjacency graph (RAG) for segmenting orientation fields is proposed. Finally, a study of the algorithm to compute the line-segment and the orientation function is analyzed.


**Figure 1. (a), (b) Fingerprint and Pearlitic images**

## 2 Some Concepts of Morphological Filtering

Mathematical morphology is based principally on so-called increasing transformations [14, 5]. In fact, one calls morphological filter all increasing and idempotent transformation. The basic morphological filters are the morphological opening $\gamma_{\mu B}$ and the morphological closing $\varphi_{\mu B}$ with a given structuring element. Here, $B$ represents the elementary structuring element containing its origin (for example a square of $3 \times 3$ pixels), $\check{B}$ is the transposed set ($\check{B} = \{-x : x \in B\}$) and $\mu$ is an homothetic parameter. Then, the morphological opening and closing are given:

$$\gamma_{\mu B}(f) = \delta_{\mu\check{B}}(\varepsilon_{\mu B}(f)) \quad \text{and}$$

$$\varphi_{\mu B}(f) = \varepsilon_{\mu\check{B}}(\delta_{\mu B}(f)) \tag{1}$$

where the morphological erosion $\varepsilon_{\mu B}$ and dilation $\delta_{\mu B}$ are expressed by $\varepsilon_{\mu B}(f)(x) = \wedge\{f(y) : y \in \mu\check{B}_x\}$ and $\delta_{\mu B}(f)(x) = \vee\{f(y) : y \in \mu\check{B}_x\}$. $\wedge$ is the inf operator and $\vee$ is the sup operator.

Morphological directional transformations are characterized by two parameters. A structuring element L depends on its length (size $\mu$) and on its the slope (angle $\alpha$). Thus, the set of points of a line segment $L(\alpha, \mu)$ is computed by two sets of points for $\alpha \in [0, 90]$. The sets of points $\{(x_i, y_i)\}$ defined by the following expressions: if $0 \leq \alpha \leq 45$ then

$$y_i = x_i tan(\alpha) \quad for \quad x_i = 0, 1, \cdots, (\mu/2)cos(\alpha)$$

and if $90 \geq \alpha > 45$ then,

$$x_i = y_i cot(\alpha) \quad for \quad y_i = 0, 1, \cdots, (\mu/2)cos(\alpha)$$

and the set of points $\{(-x_i, -y_i)\}$. This means, the structuring element is a symmetric set $L(\alpha, \mu)$=$\hat{L}(\alpha, \mu)$. Similar expressions can be expressed for $\alpha \in (90, 180]$. Then, the morphological opening and closing are given by:

$$\gamma_{L(\alpha,\mu)}(f) = \delta_{L(\alpha,\mu)}(\varepsilon_{L(\alpha,\mu)}(f)) \quad \text{and}$$

$$\varphi_{L(\alpha,\mu)}(f) = \varepsilon_{L(\alpha,\mu)}(\delta_{L(\alpha,\mu)}(f)) \tag{2}$$

where the morphological erosion and dilation are given by: $\varepsilon_{L(\alpha,\mu)}(f)(x) = min\{f(y) : y \in L(\alpha, \mu)(x)\}$ and $\delta_{L(\alpha,\mu)}(f)(x) = max\{f(y) : y \in L(\alpha, \mu)(x)\}$

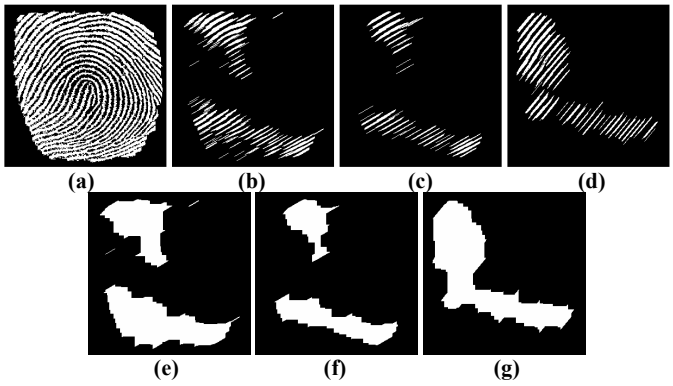


**Figure 2. (a) Original image, (b), (c) Directional openings at direction 30 degrees with size 20 and 30, respectively, (d) Directional opening at direction 50 degrees size 30, (e), (f) and (g) Morphological closings size 10 of images in 2 (b), (c) and (d), respectively.**

## 3 Size and Orientation Codification Based on Directional Erosions

In this section and in the following ones we will look for an approach where the connectivity notion plays a fundamental role for segmenting the orientation fields. In fact, it is well-known that the notion of connectivity is linked to the intuitive idea of the segmentation task, where the objective is to split the connected components into a set of elementary shapes that will be processed separately. Then, the problem lies in determining what a connected component is for an image such as those illustrated in Fig. 1. One can take different ways for introducing such a concept. For example, in Fig. 2 some orientation structures are extracted

using directional openings. Then, the orientation fields are determined by a clustering process computed in this case by a morphological closing. Figures 2 (b) and (c) show the directional openings at direction 30 degrees with sizes of the structuring elements of 20 and 30, respectively. To determine the orientation fields, the directional granulometry and a connectivity introduced by means of closings (or dilation) for extracting some clustering enable us to compute the orientation fields as illustrated in Figs. 2 (e) and (f). Nevertheless, the computing of the orientation fields by this approach can become very complex. For instance, in Figs. 2 (d) and (g) the orientation fields were determined for an angle of 50 degrees and a scale of 30. Some regions of the orientation fields of the images in Figs. 2 (c) and (f) are the same than those of the images in Figs. 2 (d) and (g) (i.e., the intersection between these images is not empty). Given that deficiency, we look for another approach where the scale and direction of the structures can be easily accessible. Two functions that codify the size and the orientation are introduced below. Let us now to define the following function:

**Definition 1** *The line-segment function $Dm_X(x)$ is a transformation that associates with each pixel x of a set X the length of the longest line segment placed at point x and completely included in X.*

The goal of building this function consists in codifying the size information in such a way that local directional information can be accessed from each point of the function. The line-segment function $Dm_X$, is computed by using the supremum of directional erosions. To stock the size information for all $\lambda$ values, a gray-level image $Dm_X$ is used. Let X be a given set, one begins with a small structuring element by taking into account all orientations to compute the set $Sup_{\alpha\in[0,180]}\{\varepsilon_{L(\lambda,\alpha)}(X)\}$. One takes all points of the image that are not removed by at least one of the directional erosions. Then one increases $Dm_X$ by one at all points x belonging to the set $Sup_{\alpha\in[0,180]}\{\varepsilon_{L(\lambda,\alpha)}(X)\}$, and one continues the procedure by increasing the size of the structuring element until the structure (the image) is completely removed. In other words, the procedure continues until one has a $\lambda_{max}$ value such that $Sup_{\alpha\in[0,180]}\{\varepsilon_{L(\lambda_{max},\alpha)}(X)\} = \emptyset$. Figures 3(b) and (c) show the output images computed from the original image in Fig. 3(a) for the size values 40 and 60, respectively. As expressed before, the gray-levels of the function $Dm_X$, are the sizes of the longest lines that can be included in the structure. Whereas, for the structures that can be considered as composed as a set of lines, as those in Figs. 1(a) and (b), we assume that the the maxima of the function $Dm_X$ play a main role since they codifies the longest lines that take the whole context of the image. Thus, one knows the position of the largest structuring elements that can be included completely in the structure. However, the angles of these structuring elements (line segments) are not accessible from the image $Dm_X$. Then, let us introduce a second function associated to the line-segment function.

**Definition 2** *The orientation function $Om_X(x)$ is a transformation that associates with each pixel x of a set X the angle of the longest line segment placed at point x and completely included in X.*

Therefore, one stocks the directions of the line segments in a second image $Om_X$, called orientation function, when the line-segment function is computed. A real example (pearlitic phase micrograph) is shown in Fig. 4. The images in Fig. 4(b)-(c) illustrate the line-segment function $Dm_X$ image and the image containing the orientation $Om_X$, respectively, computed from the binary image in Fig. 4(a). These functions serve to suggest a method for segmenting images of orientation fields.

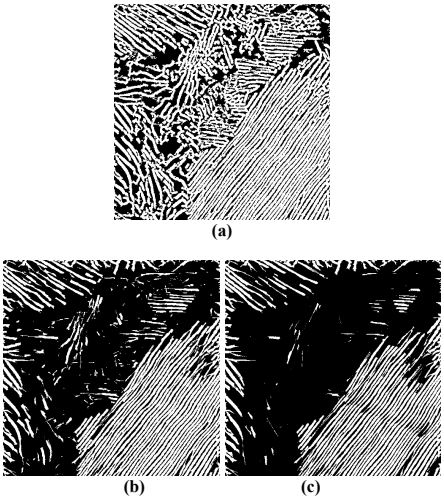


**Figure 3. (a)Original image, (b) and (c) Supremum of directional erosions size 40 and 60.**

## 4 Image Segmentation Using the Watershed Transformation and a RAG

Image segmentation is one of the most interesting problems in image processing and analysis. The main goal in image segmentation consists in extracting the regions of greatest interest in the image [4, 10]. In mathematical morphology, the watershed-plus-marker approach is the traditional image segmentation method [10]. Here, an alternative approach for segmenting images with orientation fields is applied. Instead of looking for a set of markers signaling the regions, the watershed will be applied directly to obtain

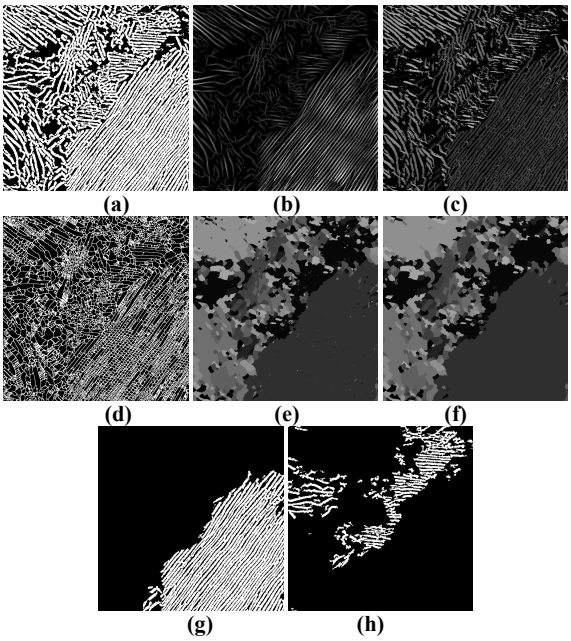


**Figure 4. (a) Original image, (b) and (c) Line-segment and orientation functions, (d) Watershed, (e) Weighted catchment basins, (f) Segmented image, (g) and (h) Connected components of (f)**

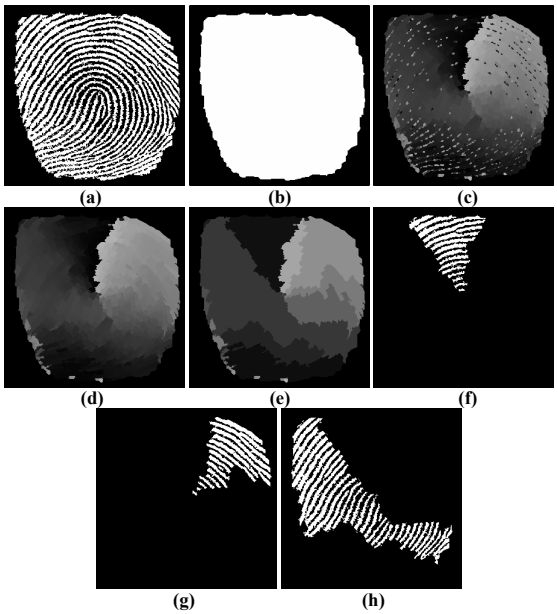


**Figure 5. (a) Original image, (b) Mask image, (c) Weighted partition, (d) filtered image by size criterion, (e) Segmented image, (f), (g) and (h) Three connected components of the segmented image.**

a fine partition. Then a systematic merging process will be applied to obtain the final segmentation. Figure 4(d) shows the the watershed computed from the inverse image of image $Dm_X$ in Fig. 4(b). To carry out the merging process it is preferable to work with the catchment basins associated with the watershed image. Figure 4(e) shows the catchment basins weighted by the values of the angles of the regional maxima of the $Om_X$ image in Fig. 4(c). Now, by analyzing a region of the image in Fig.4(e), one can identify the neighboring regions with more-or-less similar orientations. In order to take into account their neighborhood relationships, a region adjacency graph (RAG) must be computed. In fact, the RAG simplifies the merging process. We have chosen the method proposed in [15] for the merging process. Each vertex $v_i$ of the RAG corresponds a region $R_i$ with orientation values (for example, the mean value $\overrightarrow{\mu}_i$ and variance value $\overrightarrow{\sigma}_i$ of the region) representative of the orientation distribution of this region. Each edge $e_{ij}$ represents a pair of adjacent regions $\{R_i, R_j\}$ with a corresponding orientation distance $d(R_i, R_j)$, which can be used to compare the orientation distributions of these two regions. In our case, the computation of the RAG, using the angles of the regions, guides the subsequent merging of regions and provides a complete description of the neighborhoods. The RAG graph is constructed by the use of the catchment basins of the image in Fig.4(e). One takes a point from each minimum of the inverse line-segment function for representing each catchment basin. Each edge is assigned a value given by the absolute value of the difference between the angles of two neighboring regions, computed from the orientations image. The neighborhood graph of the maxima of the line-segment function $Dm_X$ and the orientation $Om_X$ function synthesize the directional field of the image. Two vertices of the graph are linked by an edge if the catchment basins are neighbors, and the value of the edge represents the directional similarity. Once the regions are codified on a graph, we can compute the orientation fields based on the valued graph. The following method (see [15]) for reducing the numbers of regions may be carried out: a) Each border has assigned an orientation distance between the two regions it separates, b) The borders are sorted in increasing order, c) Two regions separated by the smallest distance are merged, d) The step (b) is repeated until the criterion can not be satisfied. We illustrate the method by identifying the adjacent regions with more-or-less similar orientation by considering the image in Fig. 1(b), a micrograph of the pearlite structure in steel. To achieve such a goal, one merges the vertices (catchment basins) with a difference of angles smaller than or equal to a given angle value $d(R_i, R_j) = |angle(R_i) - angle(R_j)| \leq \theta$. Fig-

ure 4(f) shows the segmented image of the image in Fig. 4 (e), while Figs. 4 (g) and (h) show some connected components of the segmented image. Once the grains of the perlitic structure are separated, it is now possible to compute some measures (for example, a granulometric study). It is clear that, when the regions of the image are codified under the form of a graph, many criteria can be easily introduced to segment the image. Figure 5 shows this advantage of using a RAG structure for the merging process since the introduction of other criteria can improve the final segmentation. However, in this example, instead of computing the catchment basins on the whole image, one can do better by computing the weighted partition in a geodesic way. The mask where the catchment basins transform will be applied is given by the image in Fig. 5 (b). This is the output image obtained by the morphological closing size 6 of the original image in Fig. 5 (a). Then, the image in Fig. 5(c) is computed by the catchment basins inside the mask. Since thin connections exist between the directional structures of the orientation fields, one observes in Fig. 5 (c) small regions that are not representative of the structure (from a segmentation point of view). A size criterion was introduced to remove these regions as illustrated in Fig. 5 (d). Once the small regions are removed, two other criteria can be applied for obtaining the final segmentation. Let $\overrightarrow{\mu}_i$ and $\overrightarrow{\sigma}_i$ be the mean and the variance values in the region $R_i$. Then, two regions $R_i$ and $R_j$ can be merged if the orientation distance $d_{\overrightarrow{\mu}}(R_i, R_j) = |\overrightarrow{\mu}(i) - \overrightarrow{\mu}(j)| \leq \theta$. This means, after the merging process between regions is carried out, the mean value is used to describe the new region and a new variance value is computed. However, even if the mean difference criterion is satisfied, if one of the regions has a great variance ($\overrightarrow{\sigma}_i > \tau$ or $\overrightarrow{\sigma}_j > \tau$) , these regions will not be merged. Figure 5 (e) shows the segmented image using a mean orientation difference criterion $\theta = 15$ degrees and using a variance criterion $\tau = 5.5$. Under our approach the images in Figs. 5 (f), (g) and (h) show three connected components of the original image in Fig.5 (a), according to the image in Fig. 5(e). Compare these images, and in particular the images in Figs. 5 (f) and(h), with those of Fig. 2. From the point of view of fingerprint recognition, the connected components illustrate the existence of a singular point (core). The largest component (third connected one) describes a separation with the topmost curving that enables to classify this fingerprint. The image in 5 (e) shows clearly the existence of the core.

## 5 Non-Parametric Algorithm to Build the Line-Segment and Orientation Functions

Let us illustrate an algorithm to build the line-segment and the orientation functions that does not require any parameter and that is not expensive in computation time. First, concerning the size parameter (largest structuring element), it was fixed to the size of the image diagonal that is the size of the largest structure that can be include in the image. Let $S_x$ and $S_y$ be the dimension of the images, horizontal and vertical axis, respectively. For example, for a VGA image $640 \times 480$, one has $L = \sqrt{S_x^2 + S_y^2} = 800$, then the largest structuring element has a size of 400 since one uses symmetrical structuring elements. It is clear that few cases of images, containing such structural characteristics, can be found in real images. Next, one requires to fixe the step in degrees to compute the line segments. In practice, a step between 5 and 10 degrees is sufficiently, but let us fix it to a smaller value (one degree) in order to show the limiting case in computation time. Then, one computes 180 structuring elements of size L, and they are stocked in a structure data (list of lists). Since symmetrical structuring elements are used, only half of the straight lines is stocked and centered at origin $(0, 0)$. In fact, only the Freeman codes are stocked. Let $\{Ls_i\}$ with $i \in \{0, 1, 2, ..., 179\}$ be the lists containing the Freeman codes required to build a half of the structuring elements and let $Ls_j$ be a given list. The structuring element is built using the list $Ls_j = \{c_k\}$ with $c_k \in \{0, 1, 2, 3, ..., 7\}$ and its symmetrical data $\check{L}s_j = \{\check{c}_k\}$ with $\check{c}_k = (c_k + 4)\ mod\ 8$. Consider the example in Fig. 6(a) where an erosion by a line segment is applied to the structure in gray color. The structuring element is obtained from the list $Ls_j = \{0, 1, 0, 1, 0, 1, 0, 1, 0\}$ and $\check{L}s_j = \{4, 5, 4, 5, 4, 5, 4, 5, 4\}$. Now, to compute the erosion at point (x,y) of an image $f$ marked by a white dot, one begins by computing the smallest value between the points (x-1,y), (x,y) and (x+1,y). Then, the erosion size one is given by the infimum (the intersection for sets) $\varepsilon_1(f)(x, y) = f(x - 1, y) \bigwedge f(x, y) \bigwedge f(x + 1, y)$. Next, one computes the erosion size 2 with the following two points of the structuring element (x-2,y+1) and (x+2,y+1) and the erosion size one $\varepsilon_1(f)(x, y)$, thus, $\varepsilon_2(f)(x, y) = f(x - 2, y - 1) \bigwedge \varepsilon_1(f)(x, y) \bigwedge f(x + 2, y + 1)$. The procedure continues until the last pair of points of the structuring element is taken into account. In this example, a longer structuring element to remove the point (x,y) of the image is required. Nevertheless, in the example in Fig. 6(b), when the third erosion is applied, the point is removed by the erosion; i.e., $\varepsilon_3(f)(x, y) = f(x - 3, y - 2) \bigwedge \varepsilon_2(f)(x, y) \bigwedge f(x+3, y+3) = 0$, then, the procedure is stopped. This procedure is applied at each point of the image. It is clear that the fact of using the infimum (AND operation in a computer) to compute the erosion and to stop the procedure when it is no longer required, permits to compute the erosion of the image faster. Then, instead of calculating the $Sup_{\alpha \in [0,180]}\{\varepsilon_{L(\lambda,\alpha)}\}$, one computes at each point *x* of the image, the longest structuring element that can not remove this point. Next, the length of this structuring element is used to affect the function $Dm_X$ at point

$x$. For instance, in the example in Fig. 4(a), an image of size $512 \times 512$ pixels, 5 seconds are required to compute the line-segment and orientation images using an angle step of one degree, whereas working with a step of 5 degrees in the interval [0,180] a second is only required. For the image in Fig. 5(a) (300x300 pixels) one requires less than two seconds using an angle step of one degree. The computer, that has been used for the experiments, is a laptop with 1.59 Ghz processor and 256 MB in RAM.

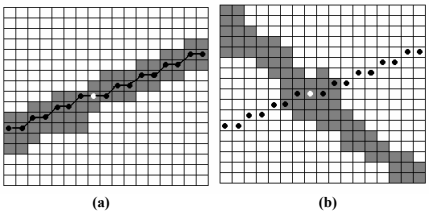


**Figure 6. (a) and (b) Directional erosions.**

## 6 Conclusion

This paper has shown the possibilities for application of morphological directional transformations to segment images with orientation fields. A local approach that involves a local analysis using the concepts of the line-segment and orientation functions is proposed in this paper. The maxima of the line-segment function were used for computing the loci of maximal structuring elements, and the orientation function was used to obtain the angles of the line segments. Then, a partition of the image may be computed by means of the catchment basins associated with the watershed transform. This enables us to realize a neighborhood analysis, using a RAG structure, in order to merge adjacent regions of the partition according to appropriate criteria, thus segmenting the images into orientation fields. The results based on the algorithms presented in this paper show the good performance of the approach.

**Acknowledgements:** Morales-Hernández thanks the government agency CONACyT for the financial support. The author I. Terol would like to thank Diego R. and Darío T.G. for their great encouragement. This work was funded by the government agency CONACyT (58367), Mexico.

## References

[1] C. Bahlmann. Directional Features in Online Handwriting Recognition. *Pattern Recognition*, 39:115–125, 2006.

[2] A. Bazen and S. Gerez. Systematic Methods for the Computation of the Directional Fields and Singular Points of Fingerprints. *Computer Vision, Graphics, and Image Processing*, 24(3):905–919, 2002.

[3] R. Cappelli and A. Lumini. Fingerprint Classification by Directional Image Partitioning. *IEEE Trans. on Pattern Anal. Machine Intell.*, 21(5):402–421, 1999.

[4] J. Crespo, R. Schafer, J. Serra, F. Meyer, and C. Gratin. A Flat Zone Approach: A General Low-level Region Merging Segmentation Method. *Signal Process.*, 62(a):37–60, 1997.

[5] H. J. A. M. Heijmans. *Morphological Image Operators*. Academic Press, New York, 1994.

[6] D. Jeulin and M. Kurdy. Directional Mathematical Morphology for Oriented Image Restoration and Segmentation. *Acta Stereologica*, 11:545–550, 1992.

[7] M. Kass and A. Witkin. Analyzing Oriented Pattern. *Computer Vision, Graphics, and Image Processing*, 37(3):362–385, 1987.

[8] J. K. Lee, T. S. Newman, and G. G. A. Oriented Connectivity-Based Method for Segmenting Solar Loops. *Pattern Recognition*, 39:246–259, 2006.

[9] J. Li, W. Y. Yau, and W. H. Constrained Nonlinear Models of Fingerprint Orientations with Prediction. *Pattern Recognition*, 39:102–114, 2006.

[10] F. Meyer and S. Beucher. Morphological Segmentation. *J. Vis. Comm. Image Represent.*, 1:21–46, 1990.

[11] L. A. Morales-Hernández, I. R. Terol-Villalobos, A. Dominguez-González, and G. Herrera-Ruiz. Characterization of Fingerprints Using Two New Directional Morphological Approaches. In *Advances on Dynamics, Instrumentation and Control*, volume II, pages 325–334. World Scientific, 2007.

[12] M. A. Oliveira and N. Leite. Reconnection of Fingerprint Ridges Based on Morphological Operators and Multiscale Directional Information. In *XVII Brazilian Symposium on Computer Graphics and Image Processing*, pages 122–129, 2004.

[13] C. H. Park, J. J. Lee, M. J. T. Smith, and K. H. Park. Singular Point Detection by Shape Analysis of Directional Fields in Fingerprints. *Pattern Recognition*, 39:839–855, 2006.

[14] J. Serra. *Image Analysis and Mathematical Morphology, Vol. II, Theoretical advances*. Academic Press, New York., 1988.

[15] L. Shafarenko, M. Petrou, and K. J. Automatic Watershed Segmentation of Randomly Textured Color Images. *IEEE Trans. on Image Processing*, 6(11):1530–1544, 1997.

[16] P. Soille, E. Breen, and J. R. Recursive Implementation of Erosions and Dilations Along Discrete Lines at Arbitrary Angles. *IEEE Trans. on Pattern Anal. Machine Intell.*, 18(5):562–567, 1996.

[17] P. Soille and H. Talbot. Directional Morphological Filtering. *IEEE Trans. on Pattern Anal. Machine Intell.*, 23(11):1313–1329, 2001.